Noise Shaping by Interval Correlations Increases Information Transfer

Maurice J. Chacron, Benjamin Lindner, and André Longtin
Department of Physics, University of Ottawa, 150 Louis Pasteur, Ottawa, Canada K1N-6N5
(Received 20 June 2003; published 25 February 2004)

The influence of intrinsic firing interspike interval correlations on the noise spectrum and information transfer is studied. This is done through the comparison of two simple firing models, one of which is a renewal process while the other displays interval correlations. These correlations are shown to shape the spike train power spectrum and, in particular, to decrease the noise power at low frequencies. Linear response theory and numerical simulations reveal how this shaping can increase the transmission of information about a time-varying signal. Our results are relevant to the analysis of nonrenewal point processes and signal detection in physics and biology.

DOI: 10.1103/PhysRevLett.92.080601 PACS numbers: 05.40.–a, 87.17.Nn, 87.19.La, 87.19.Bb

There has been much interest over the past decades in studying escape problems from metastable states [1]. In several cases, the output is a sequence of spike responses which can be described by a point process. Examples include lasers [2], photodetection [3], and neural spike trains [3,4]. In many systems, one is concerned with the statistics of the interspike intervals (ISIs) [1,5]. Most studies of excitable systems deal with first order ISI statistics such as their probability distribution. Point processes in which all second and higher order ISI correlations are zero are called renewal processes [6]. However, there is experimental evidence that many excitable systems are nonrenewal. This is the case for many neurons responding to sensory stimuli [7] including electroreceptive neurons [8,9] in electric fish that must respond to low frequency stimuli caused by prey [10]. Their firing is nonrenewal since, even in the absence of an input signal, they exhibit intrinsic nonzero ISI serial correlation coefficients defined as

$$\rho_j = \frac{\langle (I_{i+j} - \langle I_i \rangle)(I_i - \langle I_i \rangle) \rangle}{\langle (I_i - \langle I_i \rangle)^2 \rangle}, \tag{1}$$

where $\{I_i\}$ denotes the ISI sequence, j is the lag, and the average $\langle \ldots \rangle$ is performed over index i.

It has been shown that a leaky integrate-and-fire neuron with a dynamical threshold (LIFDT) could produce a spike train that displayed negative ISI correlations [9,11,12]. The action potential threshold is highly variable in neurons and can increase under repetitive firing [13]. Furthermore, numerical simulations suggest that negative ISI correlations improve the detectability of weak signals [12]. However, the actual mechanism by which intrinsic negative ISI correlations may increase information transfer is presently unknown due to the LIFDT model's complexity and to the memory carried by the threshold variable. The effects of such correlations on the spike train power spectrum and on signal transmission are the focus of our Letter. In particular, we demonstrate that this information transfer increase occurs through a reduction in the low frequency noise. Such reductions are of great interest in a variety of applications involving nonlinear oscillators, such as in Josephson junctions [5,14]. Noise shaping effects were also observed in neural networks with feedback [15], even though the dynamics were renewal.

In order to analytically explore the role of negative correlations, we use two simple spiking models, A and B. We show that models A and B have *identical* first order ISI statistics as well as *identical* linear response with respect to external stimulation. Both models are perfect integrators of the input, i.e., the observable output (e.g., the voltage across the nerve membrane for a neuron) is governed by

$$\dot{v}(t) = \mu + s(t), \tag{2}$$

where μ is a positive constant bias and $s(t)$ is a time-varying signal. Also, in both models, the threshold is drawn randomly from a uniform distribution on $[\Theta_0 - D, \Theta_0 + D]$; whenever the voltage reaches this (piecewise constant) threshold, a spike is generated and a new threshold is drawn (this is similar to previously proposed models [16]).

The models differ in their reset rules for the voltage. For model A, the voltage is decremented after spiking by the constant Θ_0 (which is the mean threshold value). Clearly, this kind of reset carries memory of the previous threshold value, thus correlating subsequent ISIs; consequently, model A generates a nonrenewal spike train. This can be seen for $s(t) \equiv 0$ considering the subintervals U_j and V_j with $I_j = U_j + V_j$ in Fig. 1: for obvious reasons we have $V_j + U_{j+1} = \Theta_0/\mu$; hence subsequent intervals are correlated via these subintervals. It is straigthforward to show that the ISI correlation coefficient is $\rho_l = \delta_{l,0} - \delta_{l,1}/2$, which is a simplified description of the negative correlation displayed by either real neurons and the more complicated LIFDT model [9,12]. Further, note that the distribution of reset values equals that of the threshold values except for the mean; i.e., reset values are distributed uniformly in $[-D, D]$.

For model B we choose a random reset $\theta_r(t)$ drawn from the uniform distribution $[-D, D]$. which is the same

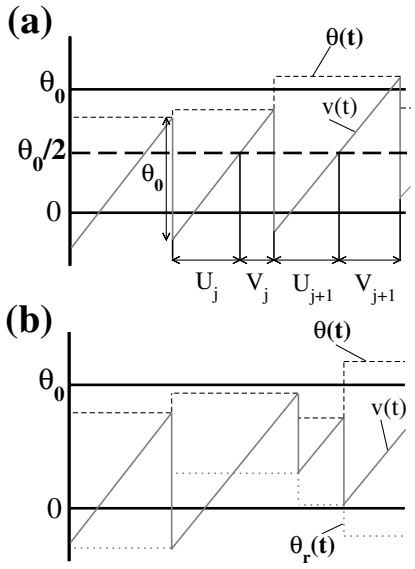

FIG. 1. (a) The dynamics of model A. Shown are the voltage $v(t)$ (solid line) which rises linearly with slope μ and threshold $\theta(t)$ (dashed line) under spontaneous activity [$s(t) = 0$]. When $v(t) = \theta(t)$, the voltage is decremented by θ_0 while the threshold is reset to a uniform random value in the interval $[\theta_0 - D, \theta_0 + D]$. Also shown are the ISI I_j that can be divided into the subintervals U_j and V_j such that $I_j = U_j + V_j$. (b) The dynamics of model B are identical to those of model A except that the voltage is reset to a uniform random value $\theta_r(t)$ (dotted line) in the interval $[-D, D]$. This eliminates memory and thus ISI correlations.

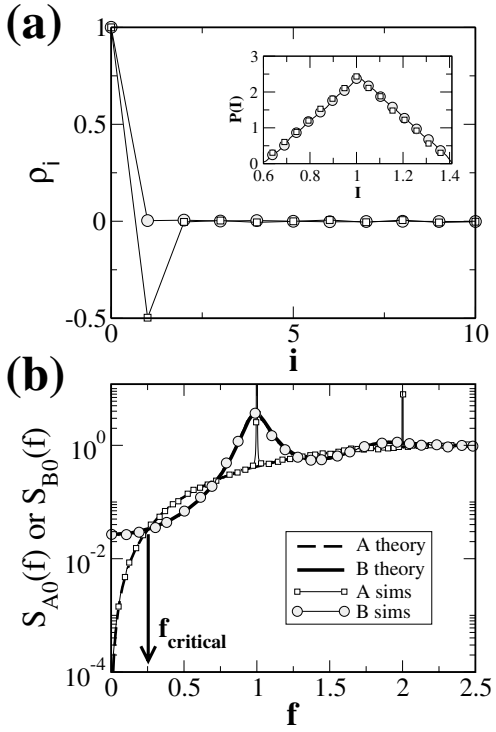

FIG. 2. Spontaneous activity of both models. (a) The ISI correlations coefficients ρ_j obtained numerically with model A (open squares) and model B (grey circles) are in excellent agreement with theoretical predictions (see text). (b) The power spectra obtained numerically with model A (open squares) and model B (grey circles) are in respective good agreement with the theoretical expressions (dashed and solid lines) given by Eqs. (3) and (4). The two spectra first intersect at f_{critical} (arrow). Simulated spectra were computed from 10^5 action potentials and averaged over nonoverlapping segments. Parameter values for numerical simulations were $\theta_0 = 1$, $\mu = 1$, $D = 0.2$, and $s(t) \equiv 0$.

as for model A. This leads to completely independent ISIs, i.e., to a renewal point process [6] with $\rho_l = \delta_{l,0}$.

We first focus on the spontaneous activity [i.e., $s(t) = 0$] of both models since most neurons that display negative ISI correlations are known to be spontaneously active in experiments [7,8]. Since the distributions of initial (reset) and final (threshold) values are the same for A and B, we obtain in both cases the same ISI density, a "triangular" function [cf. inset of Fig. 2(a)] that results from convolution of two independent uniformly distributed random numbers. Furthermore, one can determine the Fourier transforms of the density of the nth order interval (i.e., the sum of n subsequent intervals). By using these together with well-known formulas from the theory of point processes [17], one can determine the power spectra of spike trains for both models [18]. We obtain

$$S_{A0}(f) = \frac{1}{\langle I\rangle} - \frac{\sin^2(\beta f)}{(\beta f\langle I\rangle)^2}\left[\langle I\rangle - \sum_{n=-\infty}^{\infty}\delta\left(f - \frac{n}{T}\right)\right], \quad (3)$$

$$S_{B0}(f) = \frac{[(\beta f)^4 - \sin^4(\beta f)]/\langle I\rangle}{(\beta f)^4 - 2(\beta f)^2\sin^2(\beta f)\cos(2\pi\langle I\rangle f) + \sin^4(\beta f)}, \quad (4)$$

where $\beta = 2\pi D/\mu$ and the mean ISI is given by $\langle I\rangle = \Theta_0/\mu$. Both spectra are shown in Fig. 2(b) and confirmed by results of simulations. The spectrum of model A contains δ peaks at the inverse mean ISI and higher harmonics of this frequency. More interesting is the fact that the continuous background in Eq. (3) goes to zero for vanishing frequency. Both the δ peaks and the vanishing spectrum at $f \to 0$ can be understood by means of the negative correlations of model A. The power spectrum at $f = 0$ is related to the ISI correlation coefficient by $CV^2(1 + 2\sum_{i=1}^{\infty}\rho_i)/\langle I\rangle$ [6] where the coefficient of variation of the interspike interval is finite and the same for both models. Using this relation leads to a vanishing power spectrum at $f = 0$ for model A. Moreover, the ISI correlations shape the background spectrum rather than reduce the total noise power.

We investigate the consequences of these differing power spectra on information transfer by both models by studying their encoding capabilities using zero-mean band-pass limited white noise stimuli $s(t)$. Such stimuli have a power spectrum $S_{\text{st}}(f) = \alpha$ if $|f| < f_c$ and $S_{\text{st}}(f) = 0$ otherwise. Here f_c is the cutoff frequency.

Such stochastic stimuli are widely used to assess signal transmission in neurons [4,19]. Information theory [19,20] is used to quantify the amount of information that a system can transmit about these signals. For systems driven with Gaussian white noise stimuli, a lower bound on the mutual information rate can be calculated [4] as

$$\mathcal{M}_{\mathrm{A,B}} = -\int_0^{f_c} df \log_2[1 - C_{\mathrm{A,B}}(f)], \tag{5}$$

where $C_{\mathrm{A,B}}(f) \equiv |X_{\mathrm{A,B}}(f)|^2/[S_{\mathrm{A,B}}(f)S_{\mathrm{st}}(f)]$ is the coherence function; $X_{\mathrm{A,B}}(f)$, $S_{\mathrm{A,B}}(f)$ are, respectively, the cross spectrum between spike train and signal and the power spectrum of the spike train in the presence of the signal.

An evolution equation for the probability density of the voltage variable has been derived and solved in the presence of a periodic signal. This solution enables us to compute the susceptibility and to derive the power and cross spectra of the spike train in the presence of a weak signal using linear response theory [21]. We obtain

$$\begin{aligned} S_{\mathrm{A,B}}(f) &= S_{\mathrm{A0,B0}}(f) + \left(\frac{\theta_0}{\mu}\right) S_{\mathrm{st}}(f); \\ X_{\mathrm{A,B}}(f) &= \frac{\theta_0}{\mu} S_{\mathrm{st}}(f). \end{aligned} \tag{6}$$

Note that the fact that the susceptibility does not depend on frequency is a consequence of the specific noise implementation in our model [21].

We thus obtain

$$C_{\mathrm{A,B}}(f) = \left[1 + \frac{\mu^2 S_{\mathrm{A,B}}(f)}{\theta_0^2 S_{\mathrm{st}}(f)}\right]^{-1}. \tag{7}$$

The only difference in $C_{\mathrm{A,B}}(f)$ for models A and B is the baseline power spectrum $S_{\mathrm{A0,B0}}(f)$. The coherence is inversely proportional to $S_{\mathrm{A0,B0}}(f)$ which can thus be considered as a background noise spectrum that will limit the information transmission capacity. Our results demonstrate that negative ISI correlations shape the baseline spectrum and lower its value at low frequencies up to a critical frequency f_{critical} [Fig. 2(b)]. This results in $C_{\mathrm{A}}(f) > C_{\mathrm{B}}(f)$ for low f. This is verified in Figs. 3(a) and 3(b) by comparing the predictions from Eq. (7) to numerical simulations. Theoretical predictions are in excellent agreement with numerical simulations for both models. Moreover, $C_{\mathrm{A}}(f)$ approaches 1 as $f \to 0$ while $C_{\mathrm{B}}(f)$ is always less than 0.1. The former is a direct consequence of $S_{\mathrm{A0}}(f)$ approaching 0 for $f \to 0$.

Figure 4(a) compares the mutual information rate $\mathcal{M}$ computed from Eq. (5) to the one obtained from numerical simulations as a function of f_c. As expected, $\mathcal{M}$ is higher for model A than for model B. The difference $\Delta\mathcal{M} \equiv \mathcal{M}_{\mathrm{A}} - \mathcal{M}_{\mathrm{B}}$ shows a global maximum as a function of f_c. This is similar to previously reported numerical results [12] displays a frequency preference for the increase in mutual information rate. This maximum occurs for $f_c = f_{\mathrm{critical}}$ [21].

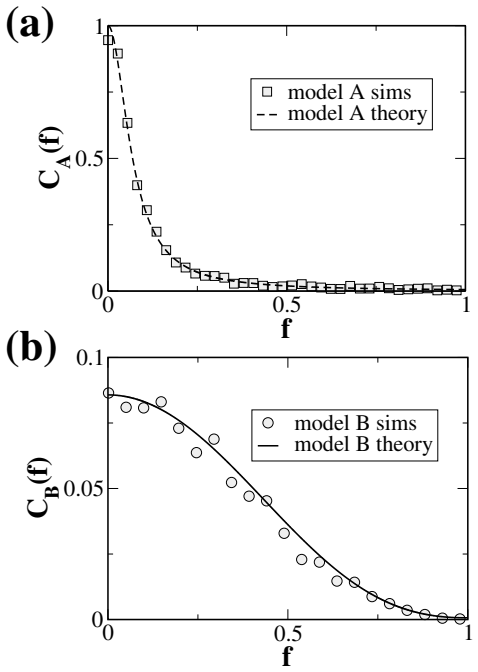

FIG. 3. (a) Coherence curves obtained numerically from model A (grey squares) and theoretically (dashed line) from Eq. (7). (b) Coherence curves obtained numerically from model B (grey circles) and theoretically (solid line) from Eq. (7). Other parameters were $\alpha = 0.0025$ and $f_c = 2$.

Figure 4(b) reveals the effects of varying the signal intensity α. As expected, the agreement between the linear response theory and numerical simulation is excellent for both models at low α. However, differences occur for higher α as nonlinear effects become important. Numerical simulations reveal that $\Delta\mathcal{M}$ decreases as α increases. This is to be expected as $S_{\mathrm{st}}(f) \gg S_{\mathrm{A0,B0}}(f)$ and the presence or absence of background noise is of little consequence. Thus, the increase in mutual information rate seems to be greatest for lower intensity stimuli. Linear response theory will fail for large f_c as it is sensitive to the signal variance $\langle \Delta s^2 \rangle = 2\alpha f_c$ [21].

We have furthermore verified the results obtained for models A and B by actual variation of the action potential threshold in a nonrenewal manner vs a purely stochastic variation in a biologically realistic Hodgkin-Huxley model. Our results show that the modification in a nonrenewal manner can give rise to negative ISI correlations as well as greater information transfer and will be presented elsewhere [21].

In summary, we have compared two simple models, one of which displayed negative ISI serial correlations and one of which did not. Both models had identical first order ISI statistics and linear response, ensuring a fair comparison without further differences (e.g., a difference

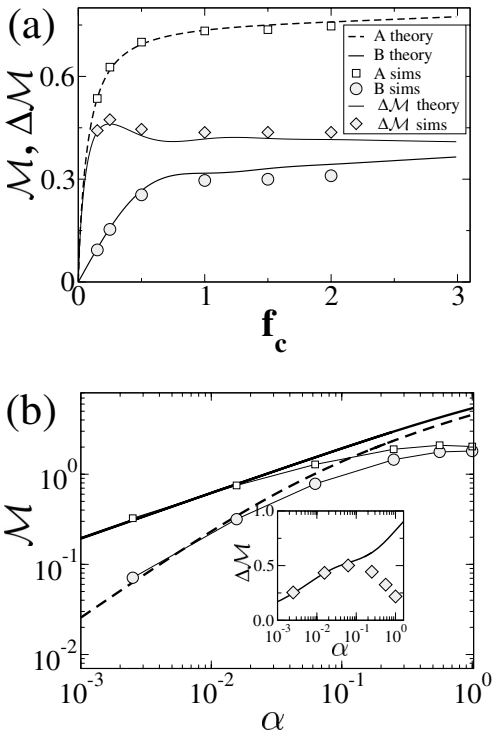

FIG. 4. (a) Mutual information rates versus cutoff frequency f_c. The numerical simulations are in respective good agreement (open squares and grey circles) with theoretical predictions (dashed and solid lines). The difference in mutual information $\Delta\mathcal{M} \equiv \mathcal{M}_A - \mathcal{M}_B$ displays a maximum as a function of f_c. We used $\alpha = 0.0156$. (b) Mutual information rates as a function of α. Numerical simulations and linear response theory show an increase in both $\mathcal{M}_A$ and $\mathcal{M}_B$ as a function of α. Linear response fails for high α. The inset shows a plot of $\Delta\mathcal{M}$ as a function of α. Numerical simulations (grey diamonds) predict a maximum in $\Delta\mathcal{M}$ as a function of α while the linear response theory (black line) predicts an increase. We used $f_c = 2$.

in firing rate would complicate the interpretation of results as mutual information is known to increase with firing rate [22]). Our calculations using linear response theory demonstrate that the noise spectrum is shaped by the negative ISI correlations without reducing the total noise power in the system. This shaping lowers the noise spectrum at low frequencies, thus enabling better information transfer. Note that our results are different from previous ones on noise shaping [15] as we are considering a nonrenewal process in a single system rather than a network of renewal processes with feedback. The gain $\Delta\mathcal{M}$ in mutual information brought on by ISI correlations was shown to be a nonmonotonous function of signal intensity α and cutoff frequency f_c. Our results suggest that such a mechanism might be at work in electroreceptive neurons of weakly electric fish. Such mechanisms may exist in other excitable systems.

We thank J. W. Middleton and L. Maler for useful discussions. This research was supported by NSERC and by CIHR.

[1] P. Hänggi, P. Talkner, and M. Borkovec, Rev. Mod. Phys. **62**, 251 (1990); L. Gammaitoni, *et al.*, Rev. Mod. Phys. **70**, 223 (1998).
[2] T. Heil, I. Fischer, and W. Elsasser, Phys. Rev. A **58**, R2672 (1998).
[3] S. B. Lowen and M. C. Teich, Phys. Rev. A **43**, 4192 (1991).
[4] F. Rieke *et al.*, *Spikes: Exploring the Neural Code* (MIT Press, Cambridge, MA, 1996).
[5] A. M. Yacomotti *et al.*, Phys. Rev. Lett. **83**, 292 (1999).
[6] D. R. Cox and P. A. W. Lewis, *The Statistical Analysis of Series of Events* (Methuen, London, 1966).
[7] K. Schäfer *et al.*, Eur. J. Physiol. **429**, 378 (1995); J. M. Goldberg and C. Fernández, J. Neurophysiol. **34**, 635 (1971); J. M. Goldberg and D. D. Greenwood, J. Neurophysiol. **29**, 72 (1966); A. Neiman and D. F. Russell, Phys. Rev. Lett. **86**, 3443 (2001); S. Bahar *et al.*, Europhys. Lett. **56**, 454 (2001).
[8] R. Ratnam and M. E. Nelson, J. Neurosci. **20**, 6672 (2000).
[9] M. J. Chacron *et al.*, Phys. Rev. Lett. **85**, 1576 (2000).
[10] M. E. Nelson and M. A. MacIver, J. Exp. Biol. **202**, 1195 (1999).
[11] C. D. Geisler and J. M. Goldberg, Biophys. J. **6**, 53 (1966); Y. H. Liu and X. J. Wang, J. Comp. Neurosci. **10**, 25 (2001).
[12] M. J. Chacron, A. Longtin, and L. Maler, J. Neurosci. **21**, 5328 (2001).
[13] R. Azouz and C. M. Gray, J. Neurosci. **19**, 2209 (1999).
[14] M. S. Sherwin and A. Zettl, Phys. Rev. B **32**, 5536 (1985); K. Wiesenfeld and I. Satija, *ibid.* **36**, 2483 (1987).
[15] D. Maar *et al.*, Proc. Natl. Acad. Sci. U.S.A. **96**, 10 450 (1999).
[16] G. Gestri, H. A. K. Masterbroek, and W. H. Zaagman, Biol. Cybern. **38**, 31 (1980); F. Gabbiani and C. Koch, Neural Comput. **8**, 44 (1996); W. Gerstner, Neural Comput. **12**, 43 (2000).
[17] A. V. Holden, *Models of the Stochastic Activity of Neurones* (Springer-Verlag, Berlin, 1976), p. 95.
[18] The power spectrum is given by $S(f) = [1 + \sum_{i=1}^{\infty}(F_n(f) + F_n(-f))]/\langle I\rangle$, where $F_n(f)$ is the Fourier transform of the nth order ISI density. The nth order ISI is given by $t_n = \sum_{i=1}^{n}(U_i + V_i)$. For model A, we have $t_n = n\theta_0/\mu + X$ with X having a triangular probability distribution in $[-2D, 2D]$. For model B, U_i and V_i have uniform probability densities and we have $F_n(f) = F_1(f)^n$.
[19] A. Borst and F. Theunissen, Nat. Neurosci. **2**, 947 (1999).
[20] R. Shannon, Bell Syst. Tech. J. **27**, 379 (1948); T. Cover and J. Thomas, *Elements of Information Theory* (Wiley, New York, 1991).
[21] B. Lindner *et al.* (to be published).
[22] A. Borst and J. Haag, J. Comp. Neurosci. **10**, 213 (2001).

Erratum: Noise Shaping by Interval Correlations Increases Information Transfer [Phys. Rev. Lett. 92, 080601 (2004)]

Maurice J. Chacron, Benjamin Lindner, and André Longtin

(Received 26 May 2004; published 28 July 2004)

DOI: 10.1103/PhysRevLett.93.059904 PACS numbers: 05.40.–a, 87.17.Nn, 87.19.La, 87.19.Bb, 99.10.Cd

We made some typing errors in Eqs. (6) and (7). The correct Eq. (6) reads

$$S_{\mathrm{A,B}}(f) = S_{\mathrm{A0,B0}}(f) + \left(\frac{1}{\Theta_0}\right)^2 S_{\mathrm{st}}(f), \qquad X_{\mathrm{A,B}}(f) = \frac{1}{\Theta_0} S_{\mathrm{st}}(f), \tag{1}$$

while the correct Eq. (7) is given by

$$C_{\mathrm{A,B}}(f) = \left[1 + \frac{\Theta_0^2 S_{\mathrm{A0,B0}}(f)}{S_{\mathrm{st}}(f)}\right]^{-1}. \tag{2}$$

For the numerical calculations we used these correct expressions; hence, all of our results and the associated conclusions are valid.

 0031-9007/04/93(5)/059904(1)$22.50

teins. As several approved cancer drugs are inhibitors of tumour-associated kinases, such as BCR/ABL, KIT, HER-2 and the epidermal growth factor receptor, the search for mutated kinases is important. Another mutated kinase is BRAF, identified in a large-scale DNA-sequencing project to be altered in melanomas (reviewed in ref. 4). But an ongoing project to sequence the genes encoding 478 kinases in a panel of breast cancers has yet to replicate the success of the BRAF example (M. Stratton).

A new way to discover the roles of particular genes in cancer is to use cultured cancer cells and the technology of RNA interference to decrease gene expression. Several academic centres and corporations are developing libraries of RNA interference reagents that reduce the expression of any of the 30,000 human genes (G. Hannon, Cold Spring Harbor Laboratory; see also page 375). These libraries will make it possible to identify the functions of genes that control crucial properties of cancer, and could therefore be attractive drug targets. Moreover, several other approaches to the development of cancer treatments are being launched. When specific target proteins are not known, gene-expression profiles may be used to screen for drugs that modulate cancer-cell behaviour (T. Golub)[5]. For example, the expression pattern of five genes distinguishes leukaemic cells from normal blood cells and can be used as a readout to search for drugs that induce leukaemic cells to differentiate[5].

Roughly 500 new anticancer drugs are in clinical trials, and many more should soon be under development as a result of new technologies. At the same time, advances in the molecular profiling of tumours could help to define diagnostic patterns that identify those patients most likely to benefit from the new treatments. Although numerous challenges still lie ahead, the future of personalized cancer treatment looks promising. ■

Olli Kallioniemi is at the Medical Biotechnology Unit, VTT Technical Research Centre of Finland, and the University of Turku, FIN-20521 Turku, Finland.
e-mail: olli.kallioniemi@vtt.fi

1. van't Veer, L. J. *et al. Nature* **415,** 530–536 (2002).
2. Van de Vijver, M. J. *et al. N. Engl. J. Med.* **347,** 1999–2009 (2002).
3. Alexe, G. *et al. Proteomics* **4,** 766–783 (2004).
4. Futreal, P. A. *et al. Nature Rev. Cancer* **4,** 177–183 (2004).
5. Stegmaier, K. *et al. Nature Genet.* **36,** 257–263 (2004).

Signal processing

Neural coding by correlation?

Arun V. Holden

Noise limits the efficiency of information transfer. But correlations of the intervals between signal pulses can reduce low-frequency noise and thereby increase the transfer of information.

A nerve cell is an example of a system whose excitation codes and transmits dynamic information. When a stimulus is above a given threshold, the neuron responds by generating an action potential, so that over time it fires irregular sequences of all-or-nothing spike responses. The ionic cell mechanisms that generate the spike are understood, but there are many mechanisms for coding the spike train, and our knowledge of these mechanisms ranges from well established to speculative. In *Physical Review Letters*, Chacron *et al.*[1] show, using a simple action-potential model, that correlations between sequential interspike intervals can shape the noise spectrum — and that this shaping can increase the transmission of information, because it reduces the noise spectrum at low frequencies.

Information theory is essentially linear[2]: a reaction is directly proportional to an action. So it might be expected that the constraints imposed by interval correlations would reduce the transmission of information. However, spike generation is a strongly nonlinear, excitable process with a threshold, and such systems can behave counter-intuitively. A good example is stochastic resonance[3], in which additive noise can increase, rather than decrease, the efficiency of information transmission.

A spike train can be represented by the sequence of intervals between spikes; this is characterized by the interval statistics (in the time domain by probability distributions and correlations, and in the frequency domain by spectral densities). Chacron *et al.*[1] consider two schemes of spike generation. The first produces a 'renewal process' that has no memory of the excitation because the system resets itself each time a spike is generated. Here, there is no correlation between successive spike intervals. The probability distributions for higher-order intervals (say, between one spike and the third spike following) and the 'autocorrelation' (the probability of a spike occurring after some other spike, irrespective of how many intervening spikes there were) can be calculated directly from the interspike-interval probability density.

The second scheme generates a non-renewal spike train, with correlations between adjacent intervals. Spike trains of sensory neurons[4] with a constant stimulus often show dependencies between neighbouring intervals; such dependencies are produced either by fluctuations in an oscillatory spike-generator or by activity-dependent changes in threshold. Long intervals followed by short ones (and vice versa) result in negative interval correlations.

The essence of spike generation is that inputs too weak to trigger a response are summed, giving a potential; when the potential reaches a threshold, a spike is generated. Chacron *et al.*[1] use a 'perfect integrator model'[5] for both spike-generation schemes, with a random threshold drawn from a uniform distribution. When the threshold is reached the potential is reset, either by an amount dependent on the magnitude of the threshold just reached (to produce serial correlation), or by a random amount (to generate a spike train with the same inter-spike-interval density but no correlation).

The advantage of using this simple model is that the spectra, coherence and information transmission rates (mutual information rates) can all be calculated, as well as estimated through computer simulation. Chacron *et al.* demonstrate that a negative serial correlation between spikes reduces the spike-train spectrum and coherence at very low frequencies, although at middle-range frequencies the coherence is increased. Serial correlation also enhances the ability of the model to transmit information by reducing low-frequency noise compared with the renewal process. Such effects have been seen in more realistic neural models[6], and can be quantified in real neural spike trains; but the complexity of both of these situations had meant that the mechanism for improved information transfer was unclear.

Whether or not this increase in the information transmission rate is exploited in neural systems is an open question, as biological evolution produces systems that work well enough and are robust, without necessarily being optimally efficient. The nervous system responds to a spike train in real time and does not process it as an indefinite sequence. But the effect of correlation on the transmission rate in a single spike train might transfer to correlations between multiple spike trains: variability between different neurons could be correlated, through common inputs and feedback[7], and coupling within a population could lead to a similar reduction in variability by noise shaping[8]. ■

Arun V. Holden is in the School of Biomedical Sciences, University of Leeds, Leeds LS2 9JT, UK.
e-mail: arun@cbiol.leeds.ac.uk

1. Chacron, M. J., Lindner, B. & Longtin, A. *Phys. Rev. Lett.* **92,** 080601 (2004).
2. Borst, A. & Theunissen, F. E. *Nature Neurosci.* **2,** 947–957 (1999).
3. Jaramillo, F. & Wisenfeld, K. *Nature Neurosci.* **1,** 384–388 (1998).
4. Ratnam, R. & Nelson, M. E. *J. Neurosci.* **20,** 6672–6683 (2000).
5. Stein, R. B., French, A. S. & Holden, A.V. *Biophys. J.* **12,** 295–322 (1972).
6. Chacron, M. J., Longtin, A. & Maler, L. *J. Neurosci.* **21,** 5328–5343 (2001).
7. Azouz, R. & Gray, C. M. *J. Neurosci.* **19,** 2209–2223 (1999).
8. Marr, D. J., Chow, C. C., Gerstner, W., Adams, R. W. & Collins, J. J. *Proc. Natl Acad. Sci. USA* **96,** 10450–10455 (1999).